

# IMPACT OF GEOLOGICAL HETEROGENEITY ON EARLY-STAGE CO<sub>2</sub> PLUME MIGRATION: SENSITIVITY STUDY

M. Ashraf<sup>a</sup>, K.A. Lie<sup>a</sup>, H.M. Nilsen<sup>a</sup> & A. Skorstad<sup>bc</sup>

<sup>a</sup> SINTEF ICT, Department of Applied Mathematics, NO-0314 Oslo, Norway

<sup>b</sup> Norwegian Computing Center, NO-0314 Oslo, Norway.

<sup>c</sup> Present address Roxar Software Solutions, Lysaker Torg 45, NO-1366 Lysaker, Norway

July 15, 2010

## Introduction

Academic studies of CO<sub>2</sub> injection frequently employ simplified or conceptualized reservoir descriptions in which the medium is considered nearly homogeneous. However, geological knowledge and experience from petroleum production show that the petrophysical characteristics of potential CO<sub>2</sub> sequestration sites can be expected to be heterogeneous on the relevant physical scales, regardless of whether the target formation is an abandoned petroleum reservoir or a pristine aquifer. Geological uncertainty introduces tortuous subsurface flow paths, which in turn influence reservoir behaviour during injection. It is paramount that the effect of the geological heterogeneity is quantified by the research community. This will facilitate both improved understanding of subsurface flow at operational CO<sub>2</sub> injection sites, and allow comparison with simulated flow in ideal homogeneous models and upscaled versions of these.

Within oil recovery, the impact of geological uncertainty on production forecast has been thoroughly investigated in the SAIGUP project [3, 4, 5] focusing on shallow-marine reservoirs. To study different factors, synthetic realistic models were made and several thousand cases were run for different production scenarios. The results showed that realistic heterogeneity in the structural and sedimentological description had a strong influence on the production responses.

The main objectives of CO<sub>2</sub> storage studies are to maximize the injection volume/rate and to minimize the risk of leakage [1, 2]. The problem of CO<sub>2</sub> storage differs from oil recovery prediction not only in the objectives of study, but also in the time scales considered for the process (thousands of years compared to tens of years for CO<sub>2</sub> migration). In addition, the characteristic length scale of the flow is much larger. Working with long temporal and spatial scales and huge amounts of uncertainties poses the question of how detailed the geological description should be. The motivation of this work is mainly to address two questions related to CO<sub>2</sub> storage:

- How sensitive is the injection and early-stage migration to uncertainty and variability in the geological description?
- What simplifying assumptions are allowed in averaging the geological attributes over scales?

To this end, we use a subset of the synthetic models from the SAIGUP study to perform a preliminary sensitivity analysis for CO<sub>2</sub> sequestration in aquifers. Heterogeneity classes are defined based on different sequence-stratigraphy parameters and levels of shale barriers. We assume two-phase flow with slight compressibility for supercritical CO<sub>2</sub>. The injection scenarios are defined based on the objectives outlined above, and important responses are discussed to evaluate the efficiency and risk of the process.

## Geological descriptions

In this work we question the widespread use of simplified geological descriptions that ignore the detailed heterogeneity in modelling. Our hypothesis is that heterogeneity features like channels, barriers, sequence stratigraphy of facies, and fault intensity/geometry all have a particular effect on flow behaviour, both locally and globally, and may significantly alter the injection and migration of CO<sub>2</sub> plumes.

Sound geological classifications and descriptions of key geological features are important to give a realistic description of the sensitivity of CO<sub>2</sub> storage performance. To this end, we have selected four parameter spaces of geological variations from the SAIGUP study [3, 4, 5]. The parameters span realistic intervals for progradational shallow-marine depositional systems with limited tidal influence. In the following, we give a brief description of each.

**Lobosity:** Lobosity is defined by the plan-view shape of the shore-line. As a varying parameter, lobosity indicates the level at which the shallow-marine system is dominated by each of the main depositional

processes. Two depositional processes are considered in the SAIGUP study: fluvial and wave processes. The higher amount of sediment supply from rivers relative to the available accommodation space in the shallow sea, the more fluvial dominant the process will be. As the river enters the mouth of the sea, it can divide into different lobes and branches. Wave processes from the sea-side smear this effect and flatten the shoreline shape. Less wave effect produces more pronounced lobe shapes around the river mouths. Very high permeability and porosity can be found in the channelling branches, while dense rock with low permeability fills the space between them. Reservoir quality decreases with distance from the shore-face. We expect that the level of lobosity can have a considerable effect on the CO<sub>2</sub> injection and plume size in the aquifer. In this study, models of three levels of lobosity are used: flat shoreline, one lobe and two lobes, see Fig. 1.

**Barriers:** Periodic floods result in a sheet of sandstone that dips, thins, and fines in a seaward direction. In the lower front, thin sheets of sandstone are interbedded with the mudstones deposited from suspension. These mud-draped surfaces are potential significant barriers to both horizontal and vertical flow. In the SAIGUP domain used here, these barriers were modelled by transmissibility multipliers in three levels of coverage of barrier sheet: low (10%), medium (50%), and high (90%). We use the same variations in this study, see Fig. 1.

**Aggradation:** In shallow-marine systems, two main factors control the shape of the transition zone between the river and the basin: amount of deposition supplied by the river and the accommodation space that the sea provides for these depositional masses. One can imagine a constant situation in which the river is entering the sea and the flow slows down until stagnation. The deposition happens in a spectrum from larger grains depositing earlier in the land side to fine deposits in the deep basin. If the river flux or sea level fluctuates, the equilibrium changes into a new bedding shape based on the balance of these factors.

In the SAIGUP study those cases are considered in which, for example, the river flux increases and shifts the whole depositional system into the sea. The angle at which the transitional deposits are stacked on each-other because of this shifting, is called aggradation angle. Three levels of aggradation are modelled here: low, medium and high (Fig. 1). As we will observe later, aggradation can have a dramatic influence on the injection and migration process.

**Progradation:** The next factor varied is the progradation or the depositional-dip direction. Two types are considered here: up and down the dominant structural dip. Since the model is tilted a little, this corresponds to the lobe direction from flank to the crest or vice-versa (Fig. 1). This has a potential influence on the CO<sub>2</sub> flow from the injection point up to the crest.

**Fault:** There are three variational dimensions considered for faults in the SAIGUP study: fault type, intensity and transmissibility. However we did not include all of these variations in our work and confined this step to two transmissibilities of almost open and closed faults. Fig. 2 shows the effect of fault transmissibility on the flow pattern. Here we took the compartment type of faults of medium intensity ([3, 5]).

## Simulation workflow

A fully automated workflow was designed for this study, starting from variational parameters in the SAIGUP models and ending into comprehensive result outputs based on the objective of the work. As a first step, 54 representative cases are studied using a commercial simulator. However, the parallel aim of future work is to develop fast simulation methods that are suitable for performing thousands of runs, using e.g., a vertically-averaged formulation [6].

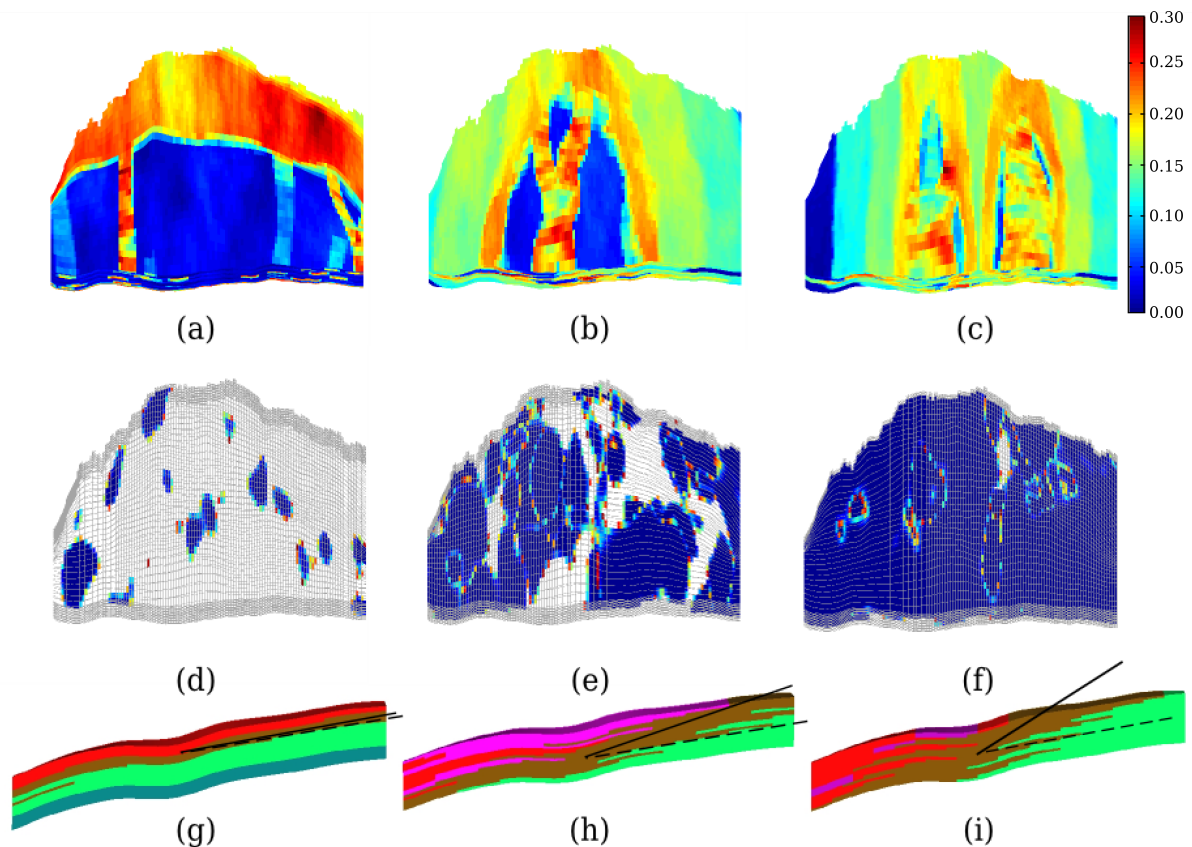


**Figure 1** Different geological features considered in this study. Top row shows 'lobosity' in porosity distribution: (a) flat shore-line, (b) one lobe, (c) two lobes. The middle row shows 'barrier' by the distribution of zero transmissibility multipliers: (d) low, (e) medium, (f) high. The lower row shows 'aggradation' in rock-type distribution: (g) low angle of interface between the transitional rock-types leads to parallel layers; this angle is increasing in cases (h) and (i), which correspond to higher levels of aggradation. An up-dip progradation direction is shown in (b), and if the lobe flips over the long axis, we will have down-dip progradation.

### Scenario design

We are using an injector down in the flank and hydrostatic boundary conditions on the sides, except the faulted side on the crest (Fig. 3). No-flow boundary conditions are imposed on the top and bottom surfaces of the model. The well is completed only in the last three layers.

Simple linear saturation functions with zero capillarity are used. This can be justified because the permeability contrast in channels has the dominating effect on the flow. Also, simple PVT data for a slightly compressible supercritical CO<sub>2</sub> is used. To model the hydrostatic boundaries in used simulator, high multipliers are used to magnify the pore volume of the outer cells in the model. About 40MM m<sup>3</sup> of supercritical CO<sub>2</sub> is injected for thirty years, which amounts to 20% of the models' pore volumes. After the injection period, seventy years of early plume migration is simulated.

### Results

As our objective function, we seek to maximize the CO<sub>2</sub> storage volume and minimize the risk of leakage. The results are discussed in three parts: first we look at model responses, then correlation between these responses. Afterwards we consider the sensitivity of each response to the studied geological feature.

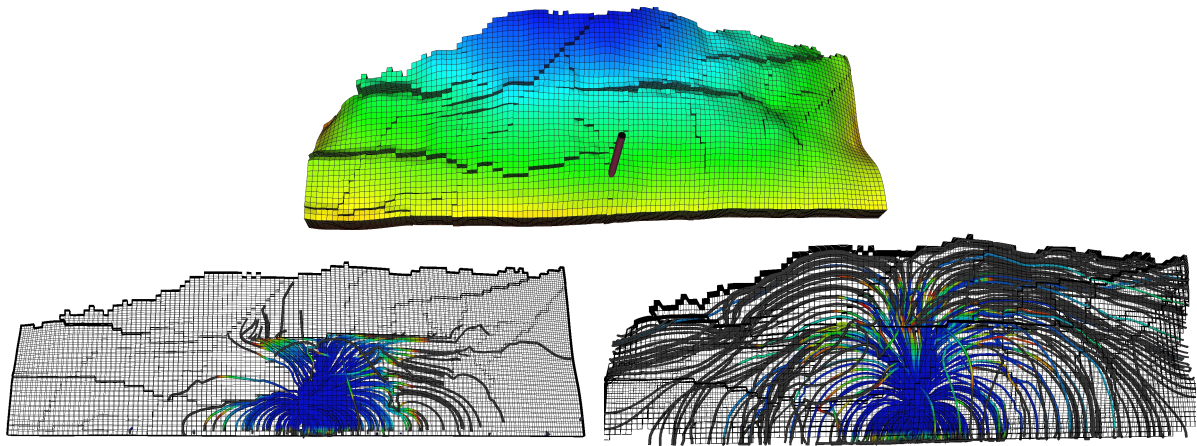


**Figure 2** The studied fault features: the picture on the top shows the orientations and intensity of the faults, down left picture shows the flow path in almost closed faults case and the one on the right is showing the flow in the almost open faulted medium. The streamlines are shown for the same time step in both pictures. Notice that the flow is confined in the closed faults model.

In all outputs, we recognize the effect of aggradation. Cases with low aggradation have continuous facies layering parallel to the horizontal direction of the grid. Because the three lowest layers, in which the well is completed, are sealing in the cross-layering direction, the flow is forced to stay in the same layers rather than accumulating in the crest (Fig. 3).

### Important responses

**Reservoir pressure:** The pressure response in general shows a sharp jump at the start of injection and a declining trend during the injection and plume migration. Pressure behaviour of different cases at the end of the injection period is shown in Fig. 4. Low aggradation cases show higher pressure.

**Boundary fluxes:** The flux out of the open boundaries is a measure of the sweep efficiency of the CO<sub>2</sub> plume. As channelling can lead to early CO<sub>2</sub> breakthrough at boundaries, we prefer cases with less fluxes out of the boundaries. The down boundary that is closer to the injector is a potential loss for the injected volume (Fig. 5(a)). Again, the flow is led to the boundaries in cases with low aggradations.

**Total mobile/residual CO<sub>2</sub>:** If the CO<sub>2</sub> saturation is below the critical value, it will be immobile in the bulk flow, although not in the molecular sense. Less mobile CO<sub>2</sub> means less risk of leakage and more residual volumes (with saturations less than the critical) resulting from a more efficient volume sweep as preferable (Fig. 5(b)). We use critical saturation of 0.2 for both water and CO<sub>2</sub>.

**Connected CO<sub>2</sub> volumes:** To estimate the risk of leakage from the cap-rock, we assume that all mobile CO<sub>2</sub> connected to a leakage point will escape out of the reservoir. Hence, it is preferable if the total mobile CO<sub>2</sub> volume is split into smaller plumes rather than forming a big mobile plume. Though the area exposed to potential leakage points will increase by splitting the plume, yet the volume reduction is overtaking the area effect.

On the other hand, the split CO<sub>2</sub> plumes can sweep more cross-areas than a big single plume. The no-flow faulted side can be considered to be connected to an imaginary large volume available for long-term plume migration. Thus, it makes sense to talk about plume sweeping cross area. Larger areas leave more residual CO<sub>2</sub> in the tail of the plume. Hence, we looked at the largest plume size, the number of plumes, and other statistical parameters. The number of plumes at the end of simulation for all cases are given

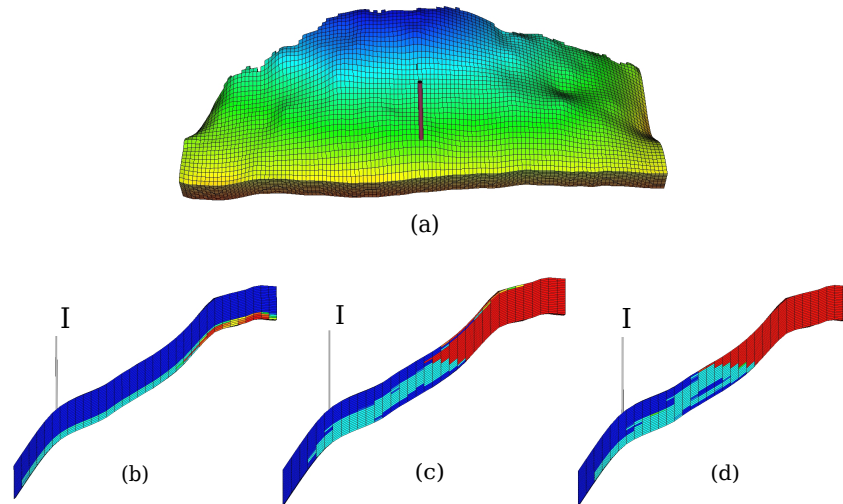


**Figure 3** (a) Model geometry and well position. Model dimensions are  $3\text{km} \times 9\text{km} \times 80\text{m}$  with 20 layers. The bottom row shows the side view of  $\text{CO}_2$  distribution (in red) at the end of simulation in different aggradation cases, from low (b) to high (d). The vertical direction is exaggerated.

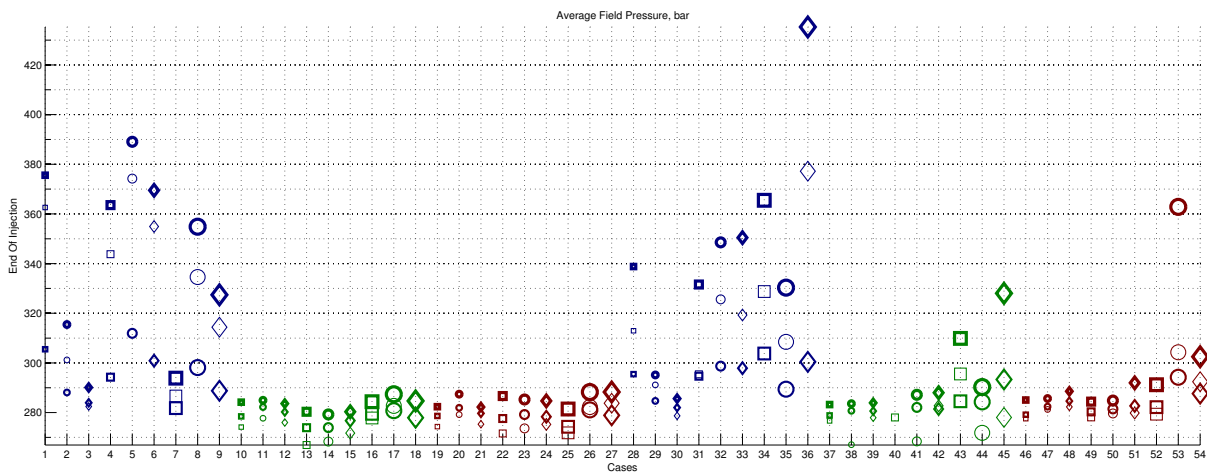


**Figure 4** Average reservoir pressure plot for all cases. Colours represent 'aggradation' level: blue for low, green for medium, and red for high levels. Size represents 'barrier': small for low, medium for medium, and large for high level of barrier. Marker shape represents 'lobosity': square for flat shore-line, circle for one lobe, and diamond for two lobes. The first half of the case numbers refer to 'progradation' up-dip towards the crest, and the second half represent 'progradation' down-dip. Thickness shows the fault criteria: thin for unfaulted, medium for open faulted and thick for closed faulted cases.

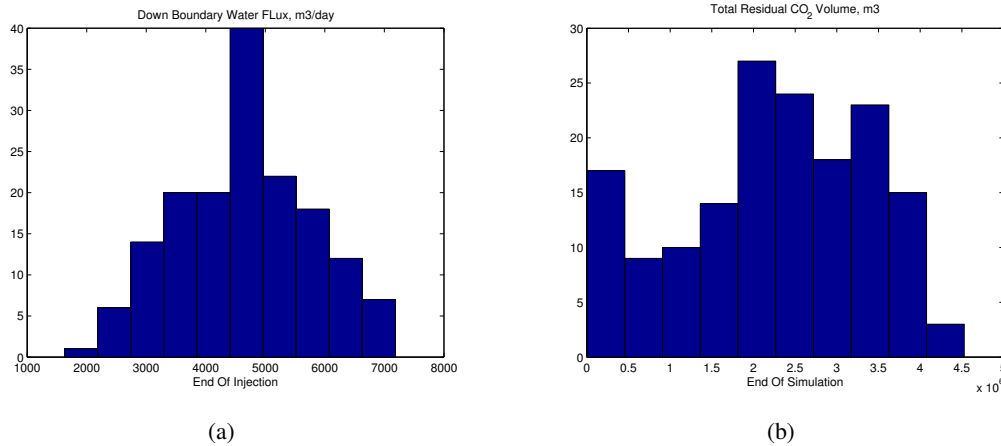


**Figure 5** (a) Flux histogram for down boundary (b) Total residual  $\text{CO}_2$  volume; cases with low aggradation show less values in a separate family.

in Fig. 7. Two-lobed cases include more branching channels which result in more plume numbers. Also barrier effect increases the lateral distribution of the plume.

### Correlation between responses

Here we relate the responses by plotting them against each other. This helps in understanding the degree of correlations between the responses. By looking at these plots we can relate the trends to geological features. This in turn helps in evaluating the effect of uncertainty of each feature on the uncertainty of the simulation outputs.

Fig. 8 shows down boundary  $\text{CO}_2$  flux versus average field pressure at the end of injection. Two linear trends can be recognized in the plot: first one starting from 280 bar going until 290 bar in a near vertical slope. The other one starts from 290 bar on the pressure axis and goes about 400 bar in a lower slope. The first trend shows that average pressure is not changing a lot with the increase of  $\text{CO}_2$  out-flux. But the second trend shows a dramatic change in pressure corresponding to the change in the down flux rate.

The second trend is made mainly by the cases of blue colour. This is again showing the effect of low aggradation in the flow and pressure behaviour. In low aggradation cases, as the  $\text{CO}_2$  flux out of the down boundary increases, the average pressure also increases in the aquifer. Effect of other geological features combined with the low aggradation dictates the amount of  $\text{CO}_2$  which goes up to the crest or stays in the bottom-most layers going out from the down boundary. Since the lower layers have poor quality rock, more flow through these layers towards down boundary result in higher pressure in the aquifer.

In Fig. 9, the total number of  $\text{CO}_2$  plumes are plotted against total residual  $\text{CO}_2$  volumes at end of simulation. The general trend shows positive correlation between these two responses. This is consistent with our discussion in the previous section about the plume size and sweep efficiency. Split plume introduces more residual  $\text{CO}_2$ . On the other hand, there is a separation in the plotted cases based on the fault criteria. Thin signs are clustered in the lower part of the graph. The medium thickness markers are clustered on the higher part of the graph and the very thick signs are sitting in between. This implies that the unfaulted cases show higher residuals with lower number of plumes, and the open faulted cases introduce more number of plumes. This can be justified by looking at a flow pattern in unfaulted and open faulted case which are shown in Fig. 10. In the open faulted cases, the flow is more laterally distributed. The closed faulted cases restrict the plume migration in the fault compartments and this

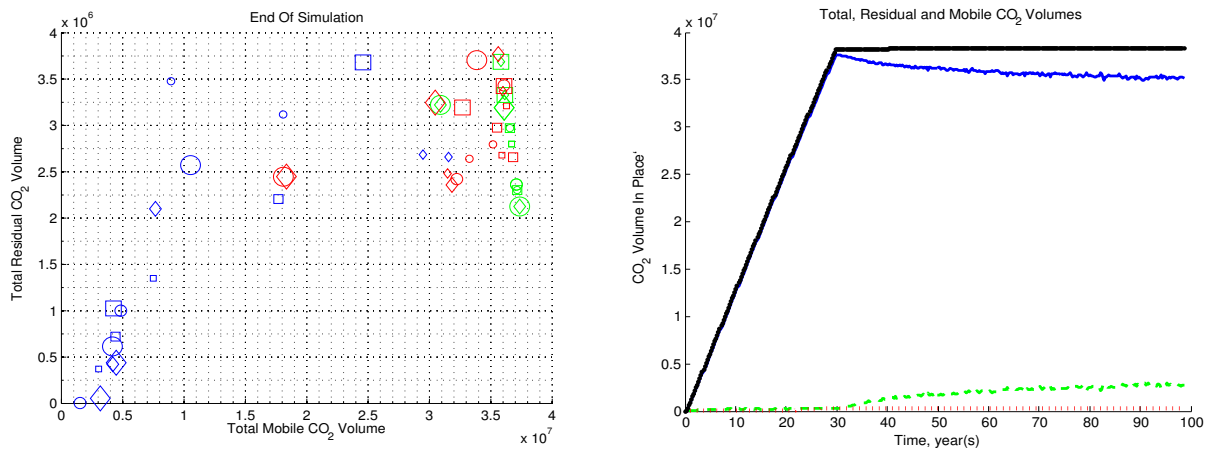


**Figure 6** CO<sub>2</sub> volumes. Left: residual versus mobile volume at the end of simulation. Most of the green coloured cases follow a linear trend, which is expected because the injected CO<sub>2</sub> must be conserved if no CO<sub>2</sub> leaves the system. For the rest of the cases, some CO<sub>2</sub> goes out of boundaries. Right: Total CO<sub>2</sub> volumes with time plotted for one case. Green curve is the residual volumes, dotted red denotes volumes that have left the domain, solid blue is mobile volumes, and the solid black shows the summation, which is the total volume and stays constant after injection because no more CO<sub>2</sub> is added to the system. The faulted cases are not included in this figure.

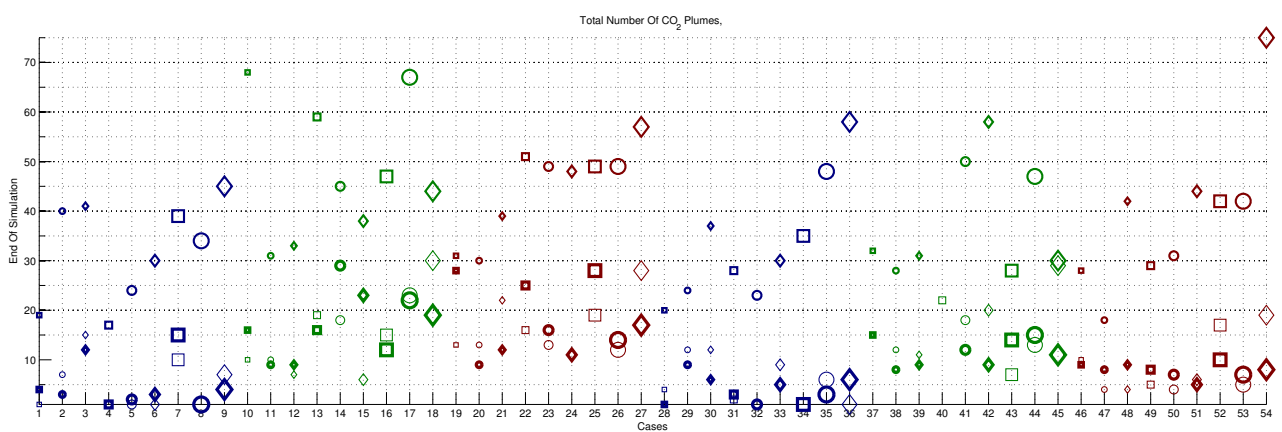


**Figure 7** CO<sub>2</sub> plume number at end of simulation, see explanation in Fig. 4.

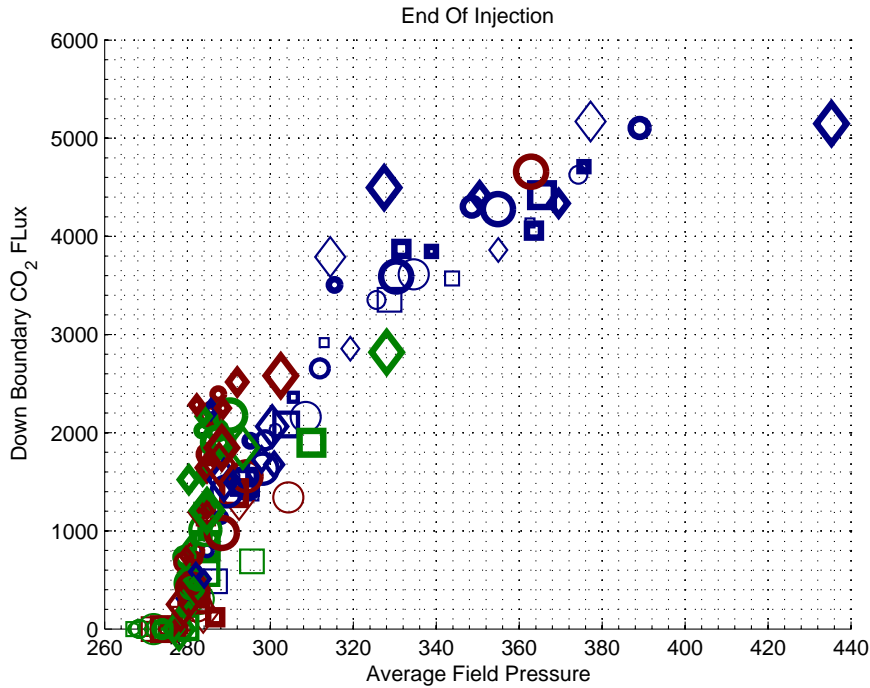


*Figure 8 Down boundary CO<sub>2</sub> flux versus average pressure, at end of injection.*

introduces lower number of plumes with lower volumes of residuals which make these cases to fall in between (Fig. 2).

Finally we look at total CO<sub>2</sub> residuals versus down boundary CO<sub>2</sub> fluxes at end of injection. We can recognize a negative correlation in an almost linear trend in Fig. 11. Higher out-flux through the down boundary leaves less CO<sub>2</sub> in the domain to migrate and this lowers the residual volumes in the domain.

### Sensitivity of responses

In this section, we try to quantify the sensitivity of flow responses to each of the geological features. To achieve this, we define a gradient for each of the features. To make it clear, we use the example of barriers which are easier to explain.

We have three levels of barrier: low, medium and high. Suppose that we are interested in calculating the gradient of average field pressure with respect to barriers. We do this in two steps: first we average the average field pressure for cases of the same level of barriers. This results in three averaged pressure values corresponding to each level of barriers. In the next step, we fit a line through these three points and calculate the tangent of this line. This represents the average pressure increase due to one level increase in barriers.

For other features like fault and lobosity, we follow the same procedure. Though the feature variation is not apparent like barrier, that points to change in the type of the feature. For example, first level of fault criteria relates to unfaulted cases, the second relates to the open faulted and the third one is for the closed faulted cases. Or regarding progradation, we have two levels: up-dip and down-dip direction. The positive and negative gradient is defined based on the way we vary the defined levels.

Fig. 12 shows the average pressure sensitivity to different features at end of injection and end of sim-

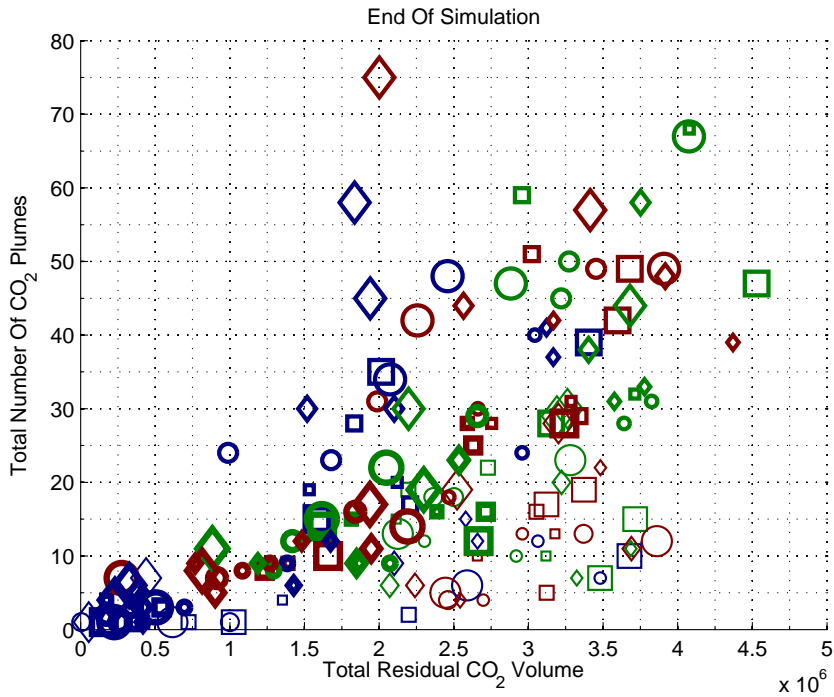


*Figure 9 Plume number versus residuals at end of simulation.*

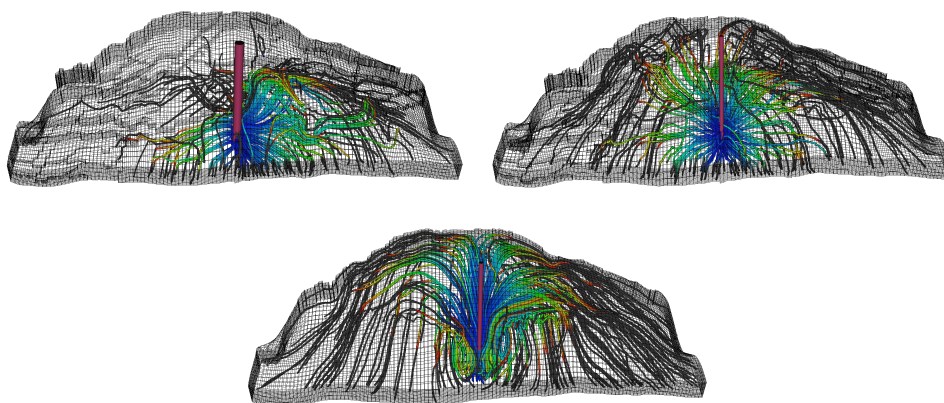


*Figure 10 Effect of fault structure on the flow pattern: top left picture shows the closed faulted case, top right picture shows the open faulted case and the bottom picture shows the unfaulted case. Open faults enhance the lateral flow, while the flow in the unfaulted case is mainly upward heading the crest.*

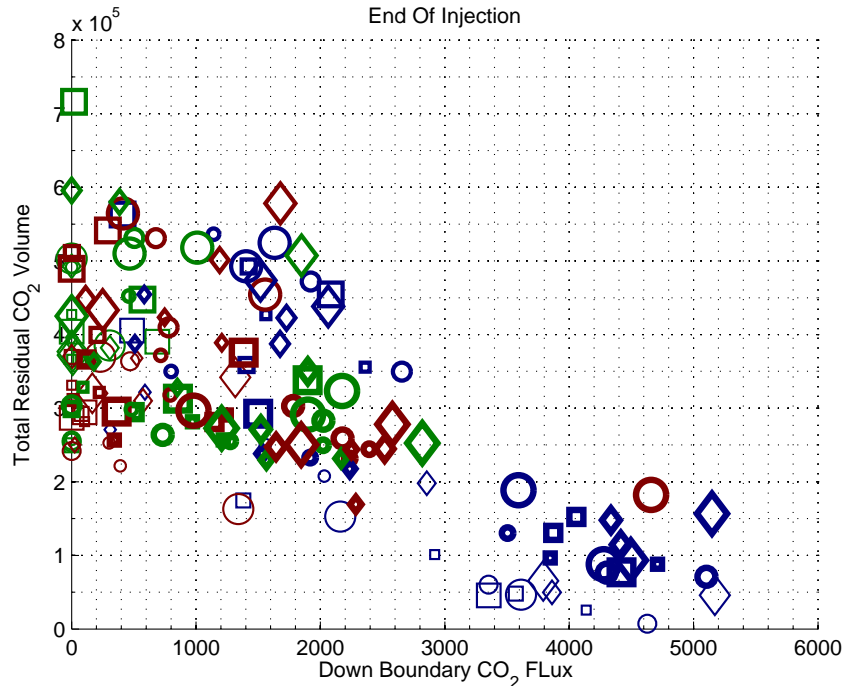


Figure 11 CO<sub>2</sub> residual volume versus down boundary CO<sub>2</sub> flux.

ulation. These results show that in the injection period the dominating effect is related to aggradation, while at end of simulation the most influential feature is the fault criteria. During injection, the flow is dictated by the viscous force imposed by the injector. This force is more sensitive to the feature. In the low aggradation cases, flow is forced to stay in the lower layers with lower permeability values. This increase the pressure in the aquifer. In the higher aggradation level, CO<sub>2</sub> can flow upward through channels with higher permeabilities. This lowers the average pressure in the domain. This is why the gradient is negative for aggradation at end of injection, since lower aggradation level introduces higher pressure.

After stopping the injection, the dominating force is the gravity. The main flow direction is vertical and the pressure is now more sensitive to fault criteria. This is what we see in Fig. 12(b).

The effect of progradation switches from positive to negative after stopping the injection. During injection period, injecting in up-dip direction is easier than injecting in down-dip direction, while for the plume migration after injection the down-dip opens more conductive medium in front of the plumes moving towards the crest.

In Fig. 13 plume number sensitivity is shown. During injection (Fig. 13(a)), barriers are the most influential features. They enhance the lateral flow and the plume splits rather than accumulating in the crest. At end of simulation (Fig. 13(b)), progradation plays an important role relatively. Note that at this time, the open faults are introducing large number of plumes, while the unfaulted and closed faulted cases introduce small number of plumes which in average cancels out to a low gradient.

Finally Fig. 14 shows gradients for total CO<sub>2</sub> residuals. During injection (Fig. 14(a)) aggradation is the most influential feature. Fault criteria is playing the most important role in the plume migration period after injection (Fig. 14(b)).

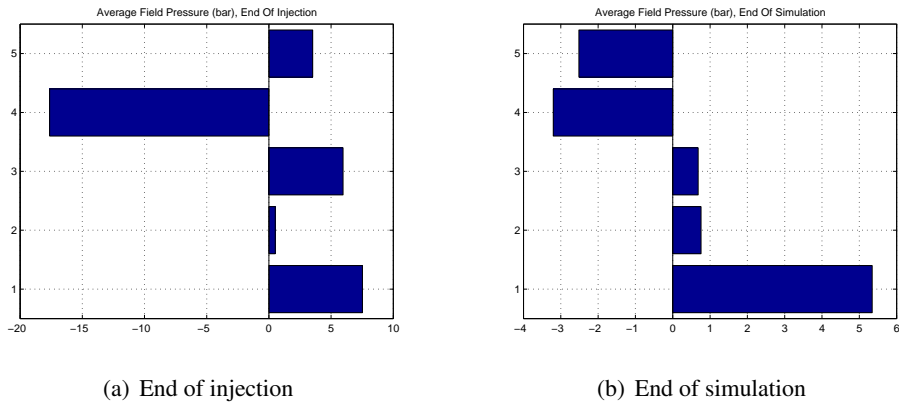


**Figure 12** Average pressure sensitivity to different geological features. In these pictures, the vertical axis shows the different geological features from bottom to top: 1-fault, 2-lobosity, 3-barrier, 4-aggradation and 5-progradation. Notice the different range in the horizontal axis at end of injection and end of simulation.

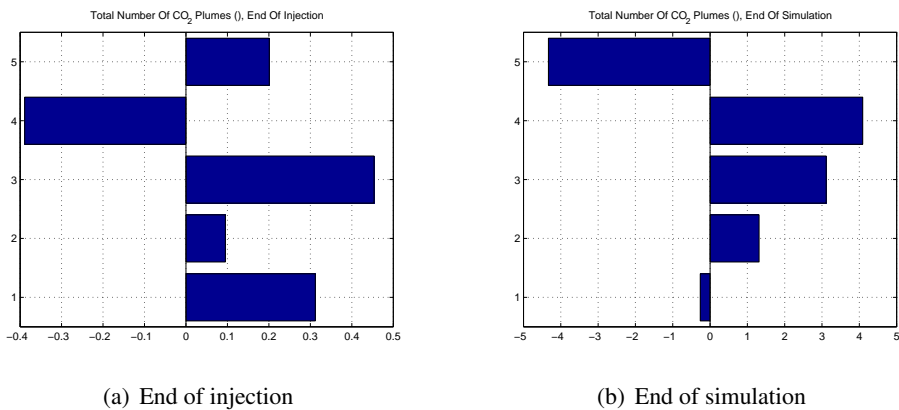


**Figure 13** CO<sub>2</sub> plume number sensitivity to different geological features. See Fig. 12 for the vertical axis explanation.

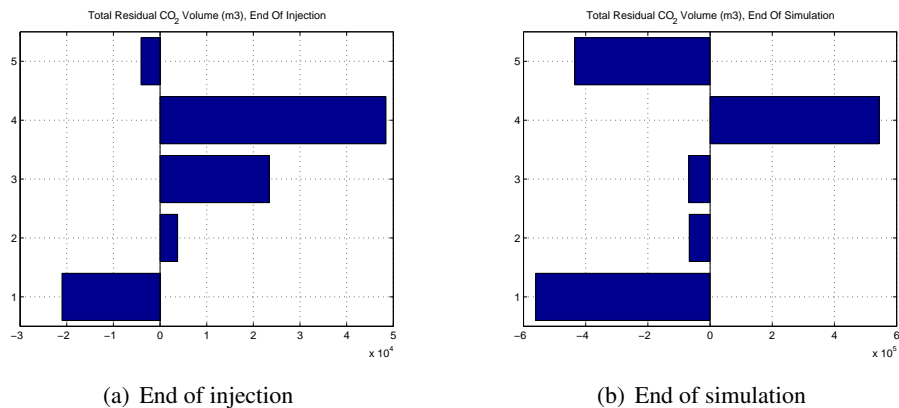


**Figure 14** Total residual CO<sub>2</sub> sensitivity to different geological features.

## Conclusions

Herein, we have reported on a preliminary study of the influence of various geological parameters on the injection and early-stage migration of CO<sub>2</sub> in progradational shallow-marine systems. The important responses related to storage capacity and risk of leakage are calculated for all the cases and discussed accordingly. The correlations between responses are investigated and a sensitivity measure is introduced and discussed for different responses.

Large variations in the flow responses show the importance of considering uncertainty in the geological parameters. Moreover, we have demonstrated that different geological parameters can have a different impact on the CO<sub>2</sub> migration during injection and during the later migration. In particular, our results highlight how variation in aggradation, fault criteria and barriers significantly change the flow direction within the medium. Therefore we believe that effort should be put into detailed geological modelling of potential injection sites. This way, one can better balance the influence of simplifications made in the models of geology and flow physics.

## References

- [1] J. M. Nordbotten: *Sequestration of Carbon in Saline Aquifers: Mathematical and Numerical Analysis*, Doctor Scientiarum Thesis, Department of Mathematics, University of Bergen, (2004).
- [2] S. Bachu: *CO<sub>2</sub> storage in geological media: Role, means, status and barriers to deployment*, Progress in Energy and Combustion Science, ELSEVIER, (2008).
- [3] J. A. Howell, A. Skorstad, A. MacDonald, A. Fordham, S. Flint, B. Fjellvoll, and T. Manzocchi: *Sedimentological parameterization of shallow-marine reservoirs*, Petroleum Geoscience, **14** (1), pp. 17-34, (2008).
- [4] T. Manzocchi, J. N. Carter, A. Skorstad, B. Fjellvoll, K. D. Stephen, J. A. Howell, J. D. Matthews, J. J. Walsh, M. Nepveu, C. Bos, J. Cole, P. Egberts, S. Flint, C. Hern, L. Holden, H. Hovland, H. Jackson, O. Kolbjørnsen, A. MacDonald, P. A. R. Nell, K. Onyeagoro, J. Strand, A. R. Syversveen, A. Tchistiakov, C. Yang, G. Yielding, and R. W. Zimmerman: *Sensitivity of the impact of geological uncertainty on production from faulted and unfaulted shallow-marine oil reservoirs: objectives and methods*, Petroleum Geoscience, **14** (1), pp. 3-15, (2008).
- [5] J. D. Matthews, J. N. Carter, K. D. Stephen, R. W. Zimmerman, A. Skorstad, T. Manzocchi, and J. A. Howell: *Assessing the effect of geological uncertainty on recovery estimates in shallow-marine reservoirs: the application of reservoir engineering to the SAIGUP project*, Petroleum Geoscience, **14** (1), pp. 33-44, (2008).
- [6] S. E. Gasda, J. M. Nordbotten, and M. A. Celia: *Vertical equilibrium with sub-scale analytical methods for geological CO<sub>2</sub> sequestration*, Computational Geosciences, **13** (4), pp. 469-481, (2009).